SMARTek
SIPIL◇ MESIN ◇ARSITEKTUR ◇ELEKTRO

URBAN FLOODS MODELLING AND TWO-DIMENSIONAL SHALLOW WATER MODEL WITH POROSITY

*Rudi Herman**

Abstrak

Pola genangan memiliki dampak yang sangat besar pada wilayah perkotaan di daerah dataran sungai. Dalam memperhitungkan perubahan dan pengurangan debit akibat adanya bangunan dan konstruksi yang lain pada wilayah dataran sungai, penggunaan model aliran dangkal dengan celah merupakan suatu hal yang diutarakan. Untuk hal ini model sumber air yang khusus untuk mengekspresikan kehilangan energi dalam wilayah perkotaan diperlukan. Formula yang diusulkan adalah membandingkan data uji coba yang diperoleh dari saluran laboratorium pada skala yang disesuaikan dengan wilayah perkotaan. Pada tingkat akurasi yang sama, metode ini memperlihatkan penurunan yang signifikan dalam perhitungannya dibandingkan dengan menggunakan grid yang lebih kecil pada simulasi klasik.

Kata kunci: *dataran sungai, model fisik, model dua-dimensi*

Abstract

Floodplains with urban areas have significant effects on inundation patterns. A shallow water model is presented, with porosity to account for the reduction in storage and in the exchange sections due to the presence of buildings and other structures in the floodplains. A specific source term representing head losses singularities in the urban areas is needed. The proposed formulation is compared to experimental data obtained from channel experiments on a scale of an urbanized area. The method is seen to result in significant reduction of computational effort compared to classical simulations using refined grids, with a similar degree of accuracy.

Keywords: *inundation, physical model, two-dimensional model*

1. Introduction

Urban areas are often vulnerable because of the conjunction of a high concentration of inhabitant and economic actors and a hazardous context (impervious areas, proximity of rivers etc). A prevention approach leads to the development of flood mapping, with various applications in the field of urban engineering: knowledge of exposure to risk, regulation of urban planning, elaboration of crisis management scenarios for example. Among the existing numerical models, two-dimensional shallow water models seem to be the best compromise between flow description, data needs and computational time. However, considering large urban areas can lead to a dramatic increase of both computational cell number and time.

The use of large-scale models in such situations constitutes an alternative, because the required detailed meshing of the urban area (to represent crossroads and squares) is bypassed through a porous zone representation. The porosity concept was first presented by Hervouet et al. [1] and Defina et al [2]. The introduction of porosity in the shallow water equation modifies the expressions for the fluxes and source terms. Following Guinot and Soares-Frazao [3], a specific source term

* Staf Pengajar Jurusan Teknik Sipil Fakultas Teknik Universitas Tadulako, Palu

representing head losses due to singularities in the urban areas (crossroads in particular) is needed. This specific source term is derived from general Borda head loss formula and takes the form of a tensor.

Depth and surface velocity measurements have been conducted over a physical model of an urban area. These experimental data are compared to various numerical simulations, including classical bi-dimensional simulation and different large-scale bi-dimensional simulations. Section 2 is devoted to a short presentation of the governing equations of large-scale models. Section 3 consists of the description of the physical model. Section 4 treats the comparison between experimental measurements and numerical results. Section 5 gives some concluding and prospective remarks.

2. Literatur Review

2.1 Governing Equations of the Numerical Model

The shallow water equations with porosity can be written in conservation form as ;

$$\frac{\partial}{\partial t}(\varphi U)+\frac{\partial}{\partial x}(\varphi F)+\frac{\partial}{\partial y}(\varphi G)=S \quad \text{....(1)}$$

$$U=\begin{bmatrix} h \\ hu \\ hv \end{bmatrix},\quad F=\begin{bmatrix} hu \\ hu^2+gh^2/2 \\ huv \end{bmatrix},\quad G=\begin{bmatrix} hv \\ huv \\ hv^2+gh^2/2 \end{bmatrix},\quad S=\begin{bmatrix} 0 \\ S_{0,x} \\ S_{0,y} \end{bmatrix}+\begin{bmatrix} 0 \\ S_{f,x} \\ S_{f,y} \end{bmatrix}$$

……..……(2)

Where g is the gravitational acceleration, h is the water depth, u and v are the x- and y- velocities respectively, ϕ is the porosity, $S_{o,x}$ and $S_{o,y}$ are the topographical source terms arising from the bottom slopes and porosity variations in the x- and y- directions respectively, S_{fx} and S_{fy} are the source terms arising from energy losses in the x- and y- directions, respectively [3].

In what follows, ϕ is assumed to depend on the space coordinates only. The topographical source terms can be written as :

$$\begin{bmatrix} S_{0,x} \\ S_{0,y} \end{bmatrix}=\begin{bmatrix} -\phi g h\dfrac{\partial z_b}{\partial x}+g\dfrac{h^2}{2}\dfrac{\partial \phi}{\partial x} \\ -\phi g h\dfrac{\partial z_b}{\partial y}+g\dfrac{h^2}{2}\dfrac{\partial \phi}{\partial y} \end{bmatrix} \quad \text{.....(3)}$$

where z_b is the bottom elevation. The first term on the right-hand side eq. (3) accounts for variations in the bottom level. The resulting force on the water body is exerted only a fraction ϕ of the total section of the control volume. The second term on the right-hand side account for the longitudinal variations in the porosity. The energy losses term is assumed to result from (i) the bottom and wall shear stress, accounted for by Strickler's law and (ii) the energy losses triggered by the flow regime variations and the multiple wave reflections due to obstacles or crossroads, accounted for by classical head loss formulation. It can be written as;

$$\begin{bmatrix} S_{f,x} \\ S_{f,y} \end{bmatrix}=-\phi g h(u_x^2+u_y^2)^{1/2}\left(\frac{1}{K^2h^{4/3}}+\begin{bmatrix} s_{xx} & s_{xy} \\ s_{yx} & s_{yy} \end{bmatrix}\right)\begin{bmatrix} u_x \\ u_y \end{bmatrix}$$

……..(4)

Where K is the Strickler coefficient assumed to be isotropic in the following, s_{xy}, s_{xy}, s_{yx} and s_{yy} are coefficients accounting for the local head losses due to urban singularities. These four coefficients involved in a tensor are necessary to represent head losses in a street network not aligned on the system coordinates, Eq. (4) reduces to;

$$\begin{bmatrix} S_{f,x} \\ S_{f,y} \end{bmatrix}=-\phi g h(u_x^2+u_y^2)^{1/2}\left(\frac{1}{K^2h^{4/3}}+\begin{bmatrix} s_x & 0 \\ 0 & s_y \end{bmatrix}\right)\begin{bmatrix} u_x \\ u_y \end{bmatrix}$$

……(5)

In what follows, Eq. (1) is discretised using the finite-volume

approach on unstructured grids with a Godunov-type scheme [4, 5]. A one-dimensional Riemann problem is defined in the local coordinate system attached to each interface. The flux vector in the direction normal to the interface is computed using the following procedure. In a first step, the Riemann problem in the global coordinate system is transformed to the local coordinates system. In a second step, the local Riemann problem is solved using a modified HLLC Riemann solver. Then the flux is transformed back to the global coordinate system. These numerical treatments are not detailed in this paper, see reference [3] for more details.

3. Description of the Physical Model

The experimental set-up is located in the laboratory of the Civil Engineering and Geoscience Department of the University of Newcastle Upon Tyne, United Kingdom. The channel is horizontal, 36 m long and 3.6 m wide, with a partly trapezoidal cross section as indicated in Figure-1. A gate is located between two impervious blocks in order to simulate a breach in a dam or a dyke. In this study, a steady flow with a discharge of 95 l/s was simulated through the breach, by maintaining the gate open. A simplified urban district is placed in the channel, with a staggered layout. The Strickler coefficient of the channel is equal to 100 $m^{1/3}/s$.

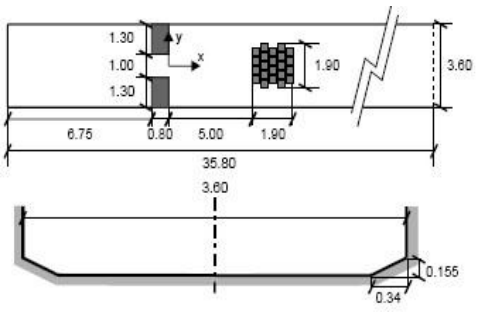

Figure-1. Experimental set-up : channel dimensions (m) and urban district layout.

4. Comparison Between Experimental Measurement and Numerical Results

Two types of numerical simulations were undertaken:

- A classical 2D simulation, where buildings are represented as impervious boundaries, and ϕ is uniformly equal to 1.
- A porosity 2D simulation, where ϕ is equal to 1 everywhere except in the urban area where ϕ is strictly less than 1. The building are not explicitly represented in this simulation.

Various values of head losses coefficients s_x and s_y were tested for representing the influence of the street network. The porosity ϕ of the urban area was calculated as the ratio of the total plane area of the buildings to the area of the square delimiting the 22 buildings. This leads to a value of 0.45.

4.1 Influence of the meshing density of the urban area

Two porosity simulations have been compared, one with a refined meshing of the urban area, and the other with a coarse one. No local head losses are involved in this paragraph. In what follows, the different simulations will be recalled by two letters acronym, the first letter indicates the simulation type (Refined or Coarse). The channel was divided into three zones, the characteristic mesh lengths of which can be found in table-1. With the PR simulation, the urban area is meshed exactly as in the CR simulation, but the inside area of the buildings is meshed too.

The free surface profiles for the three simulations were plotted along the longitudinal axis y = 0, with the experimental data (Figure-2). The dashed line represents the limits of the square bordering the 22 buildings, and the gray-filled rectangles delimit the buildings positions on the specified longitudinal axis. The Cr profile appears to be very close to represent the influence of the urban area. Two alternative solutions are conceivable, either to artificially reduce the Strickler

coefficient, or to use the local head-losses formulation of Eg. (4). The first solution is not physically appropriate because Strickler formulation is valid for turbulent shear stress within the boundary layer at the bottom and walls, whereas local head-losses are assumed to be identical over the entire flow cross-section and should therefore simply be proportional to the square of the velocities involved [3].

Table 1. Characteristic mesh, cells number and computational time for each simulation.

Description	CR	PR	PR
Upstream part	0.40 m	0.40 m	0.40 m
Downstream part except urban area	0.20 m	0.20 m	0.20 m
Urban area	0.03 m	0.03 m	0.14 m
Total cells number	10335	15299	5549
Computational time (400s simulated)	132 mn	200 mn	63 mn

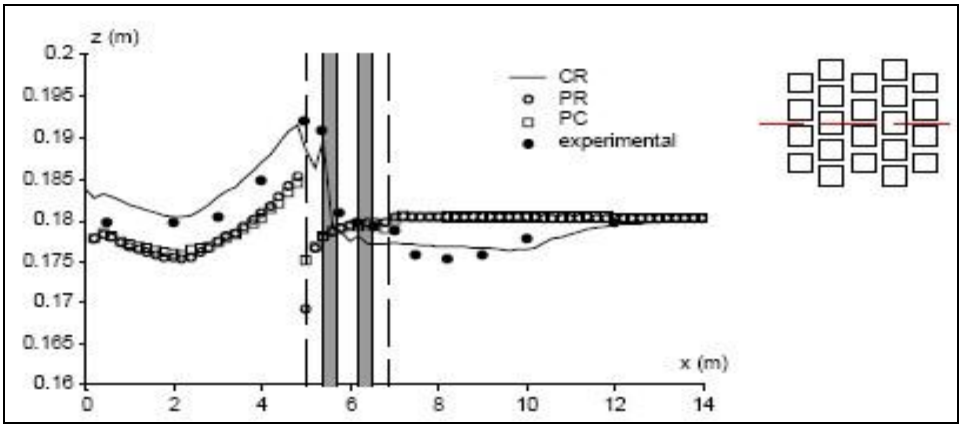

Figure 2. Simulated free surface profile without local head loss and depths along the axis y = 0

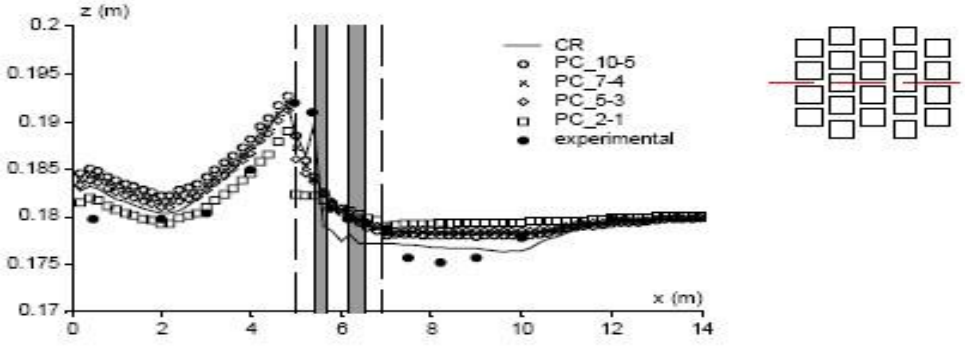

Figure 3. Simulated free surface profile without local head loss along the axis y = 0

4.2 Influence of local head losses

Simulated free surface profiles (CR and PC) were compared with the experimental data but PC simulation here involved local head-loss coefficients. The various PC simulations will be recalled by the code PC_s_x-s_y in what follows. The coefficient s_x of Eq. (5) has been fixed greater than the coefficient sy, because only the transversal streets are continuous. The computational time of all PC_s_x-s_y simulations is approximately the same as given in the table-1. The following pairs (s_x-s_y) have been tested: (10-5), (7-4), (5-3) and (2-1). All the resulting simulated profiles are very close to the CR profile and experimental depths, but PC_5-3 appears to be the closest (Figure 3).

Compared to the various paragraph results, it can be noted that the use of the local head-losses coefficient leads to a clear improvement of the simulated profile. The increase of the free surface profile before the city is well produced, but the drop after the city is under estimated. The three PC_10-5, PC_7-4, PC_5-3 simulations are very close to each other, so the sensitivity of the model to the two local head-losses coefficients is not very high.

4.3 Comparison of the velocity fields

The CR and PC_5-3 simulated velocity fields are compared to the one obtained by the digital imaging technique over the limited data acquisitions window. It appears that experimental and CR velocity fields are very similar (Figure 4). The main flow skirting the city is well simulated, as well as the re-circulation zones located next to the buildings. The secondary flows existing the city through the transversal streets seem to be well represented too. Difficulties to have tracer particles in the right lower corner of the acquisition window are responsible of the lack experimental velocities in this zone. But it seems that the extension of the re-circulation zone between the building no. 2 and no.4 is under estimated in the CR simulation.

Experimental and PC_5-3 velocity fields are obviously very different inside the urban area, because of the absence of buildings in the PC simulation (Figure-5). But it is interesting to see that the use of porosity and local head-losses makes the flow mainly escaping from the urban area.

The agreement between the experimental and the CR velocities is very good. This could be used to validate the PC simulations without the need to track the tracer particles over the entire channel. At a large scale, the velocities can be considered as correctly simulated with the PC_5-3 simulation.

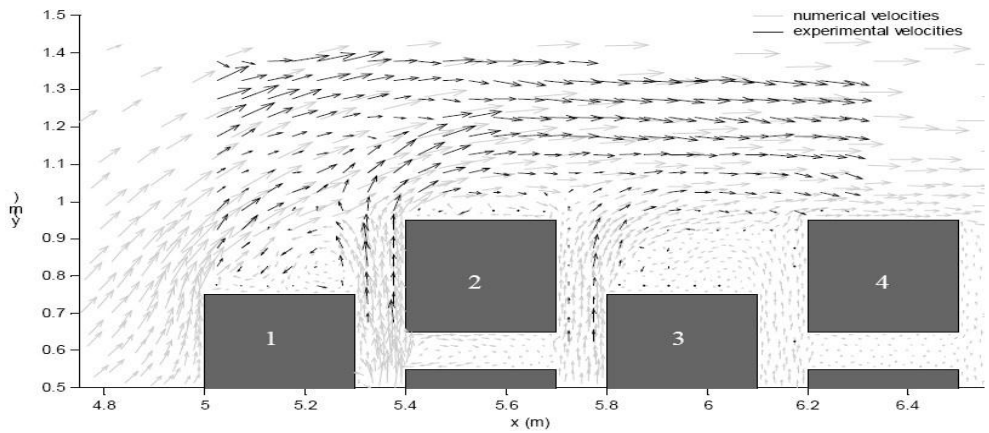

Figure 4. CR and experimental velocities fields.

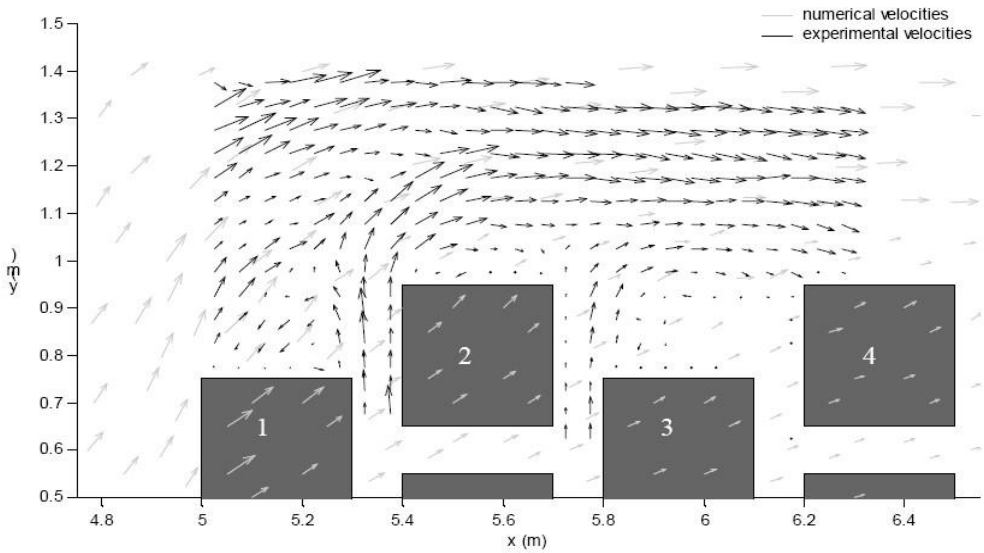

Figure 5. PC_5-3 and experimental velocities fields.

5. Conclusions

A large-scale model has been used to simulate a steady flood flow through a simplified urban area. It has been compared with both experimental depth and velocity measurements, and classical two-dimensional model.

The large-scale model gives a good description of the main features of the flow (except inside the urban area), at a much lower computational cost than classical models. This illustrates the possible operational uses of such models, (i) large-scale simulation results may be used to provide boundary conditions to local models where the details of urban areas are represented, (ii) the simulation of floodplain featuring urbanized areas, but where the details of the flow within the urban areas are not of direct interest.

Further investigations are needed to express the components of the local head-losses tensor as functions of the geometrical characteristics of the urban area: buildings density, streets width, direction and slope.

6. References

Capart H., Young D.L., Zech Y.,2002, " *Voronoi imaging methods for the measurements of granular flows*". Experiments in Fluids, Vol. 32, No.1, 2002, pp 121-135.

Devina A., D'Alpaos L., Mattichio B.,2004, " *A New Set of Equations for Very Shallow Water and Partially Dry Areas Suitable to 2D Numerical Domain*"' Proceedings Specially Conference 'Modelling of Flodd Propagation Over Initially Dry Areas' Milano, Italy.

Guinot V., Soares-Frazao S., 2006, "*Flux and Source Term Discretization in Two Dimensional Shallow-Water Models With Porosity on Unstructured Grids*". Int. Journal.'Numerical Methods in Fluids, Vol 50, No.3, (2006), pp 309-345.

Guinot V., 2003, "*Godunov-type Schemes, an Introduction for Engineers*", Elsevier, Amsterdam, The Netherlands.

Hervouet J.,M., Samie R., Moreau B., 2000, "*Modelling Urban Areas in DamBreak Flood Wave Numerical Simulations*", Proceeding of the International Seminar and Workshop on Rescue Based on Dambreak Flow Analysis, Seinajoki, Finland, (2000).

Toro E.F., 1997, "*Riemann Solvers and Numerical Methods for Fluid Dynamics*", Springer, Berlin, Germany, (1997).